

Characterization of molecular targets of the novel platinum agent PT-112 in human colon cancer cells.

Justin Wang¹, Tyler Ames², Emily Arciero¹, Marie-Therese Hehenberger³, and Devasis Chatterjee¹

¹Department of Medicine, Rhode Island Hospital and The Alpert Medical School of Brown University, Providence, RI , ²Phosplatin Therapeutics, New York, NY and ³University of Natural Resources and Life Sciences, Vienna, Austria

Background

The platinum analogs cisplatin, carboplatin and oxaliplatin are used in numerous standards of care, yet are prone to DNA-repair related acquired drug resistance as well as various toxicities, including acute and chronic neurotoxic side effects. There is a need for a more efficacious, better-tolerated platinum-based compound with novel signaling components among its mechanism of action in order to increase patient survival and quality of life. PT-112 is a novel platinum-based chemotherapeutic agent currently under clinical development that has demonstrated superior efficacy in resistant cell lines and patient-derived tumor models. Furthermore, its chemical composition leads to a significant reduction in the likelihood of promoting oxaliplatin-induced neurotoxicity, as studied separately by the sponsor. The purpose of this study was to delineate differences in the mechanism of action (MOA) when compared to oxaliplatin and to identify unique molecular targets responsible for the antineoplastic effects of PT-112. In this study we focus on the differential mechanistic effects of PT-112 and oxaliplatin treatment of HCT 116 colon cancer cells and report data derived from multiple cancer signaling pathways.

Results

Treatment of HCT 116 cells with the IC₅₀ dose of PT-112 and oxaliplatin for 24h and 48h resulted in growth inhibition and apoptosis induction as measured by MTT assay (data not shown) and PARP cleavage. At equipotent doses, oxaliplatin treatment resulted in greater DNA damage as measured by H2AX serine phosphorylation when compared to PT-112, whereas PT-112 induced markedly greater degrees of expression of several proteins in multiple pathways, including p53, p16, p21 and FasL. Additionally, PT-112 triggered the cleavage of executioner procaspases 6, 7 and 9 to a greater extent vs oxaliplatin. When compared to oxaliplatin, PT-112 treatment resulted in the significant inhibition of JAK/STAT signaling and transcriptional activation mediated by IL-6. A decrease, relative to oxaliplatin, in TNF-mediated NF-κB signaling and expression of cell-cycle factors E2F3, CDK4 and CDK1, and cell survival protein c-FLIP_{short} were also observed. PT-112 was more potent than oxaliplatin in inducing the release of High-mobility group protein B1, and the surface expression of calreticulin (CRT), markers for immunogenic cell death (ICD) processes. Additionally, the inhibition of the malignant phenotype, as assessed by anchorage independent growth, was significantly greater in cells incubated with PT-112 when compared to oxaliplatin. When treating non-malignant 1459 colon cells with concentrations equal to and higher than those used in the HCT 116 experiments, PT-112 did not result in apoptosis, exhibiting greater cancer cell selectivity than oxaliplatin.

Conclusions

PT-112's ability to affect numerous intracellular proteins, and the evidence of extracellular initiation of anticancer signaling, along with the apparent reduced dependence on DNA-damage, make it an attractive and versatile compound, particularly as it relates to potential drug resistance mechanisms. In conclusion, our study has demonstrated that PT-112 treatment simultaneously regulates multiple cellular targets including apoptosis, cell survival, tumor suppressor, and cell cycle proteins and pathways in a manner that is different from oxaliplatin. PT-112's inhibition of STAT3 activation and induction of ICD also offers the intriguing proposition of downstream immune-potentiating therapeutic effects. These results underline a unique rationale for further clinical evaluation of PT-112.

Chemical Structures

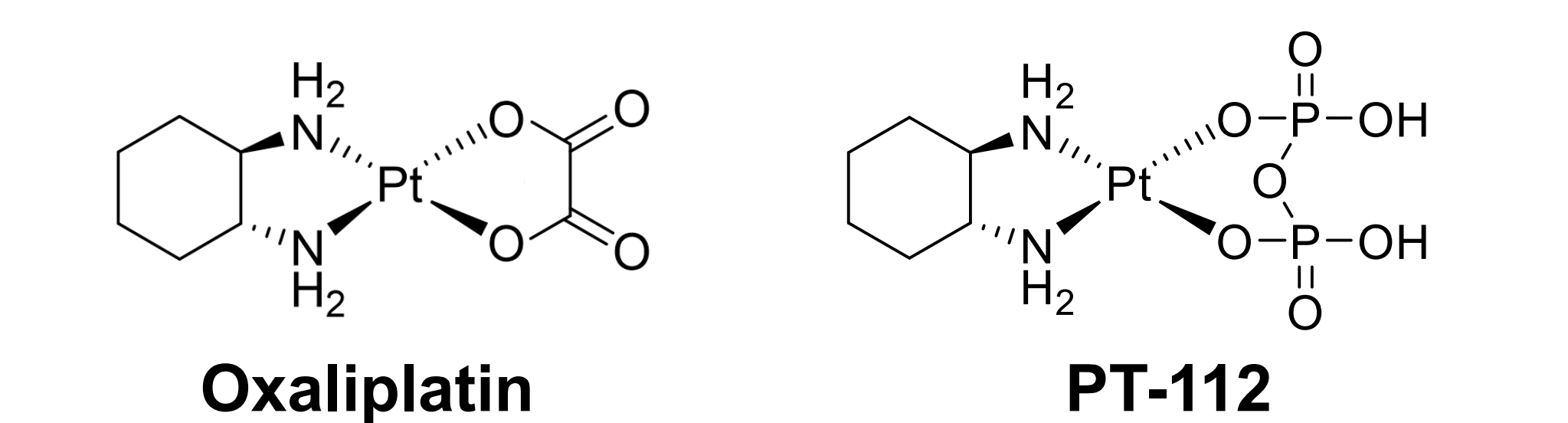


Figure 1. Chemical Structures of Oxaliplatin and PT-112.

DNA Damage and Repair

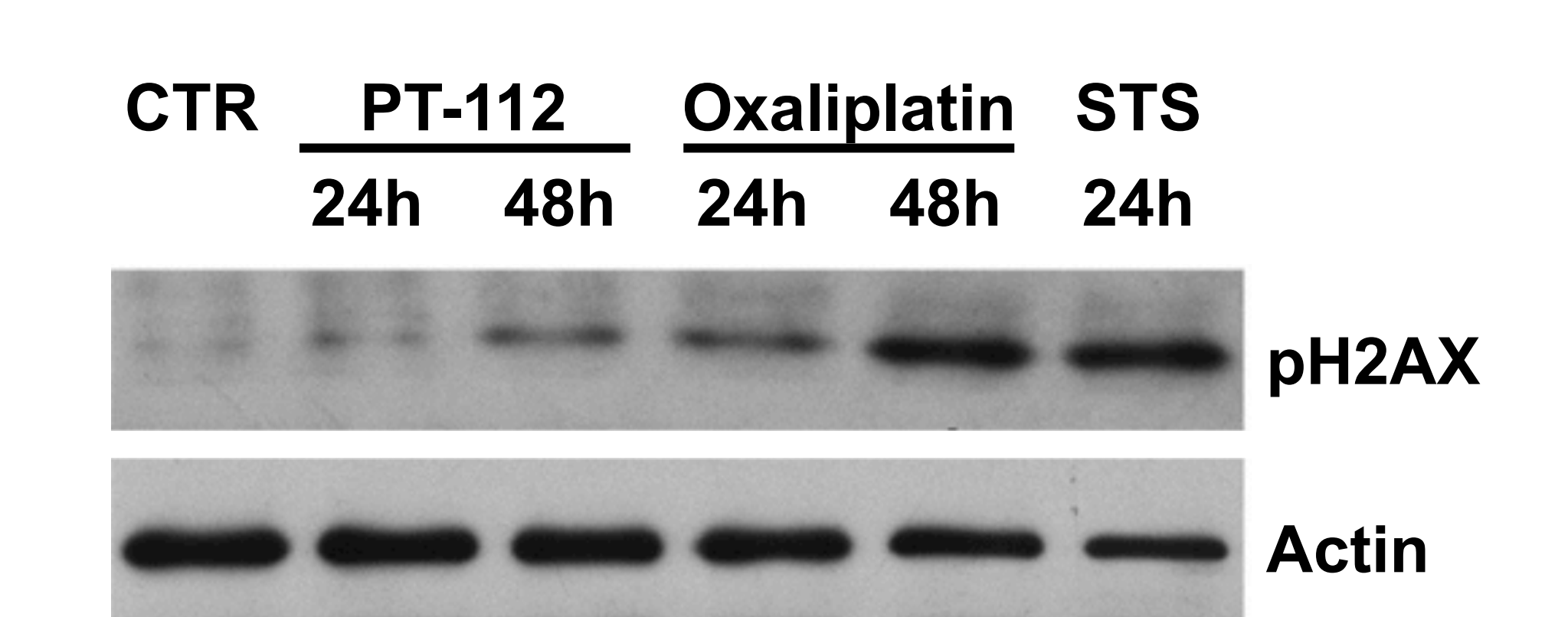


Figure 2. H2AX Phosphorylation. Western blot analysis of HCT 116 cells treated with IC₅₀ concentrations of PT-112 and Oxaliplatin for 24h and 48h and staurosporine (STS) for 24h. Enhanced levels of phosphorylated H2AX (pH2AX) indicate DNA damage and repair.

Cell Cycle Arrest

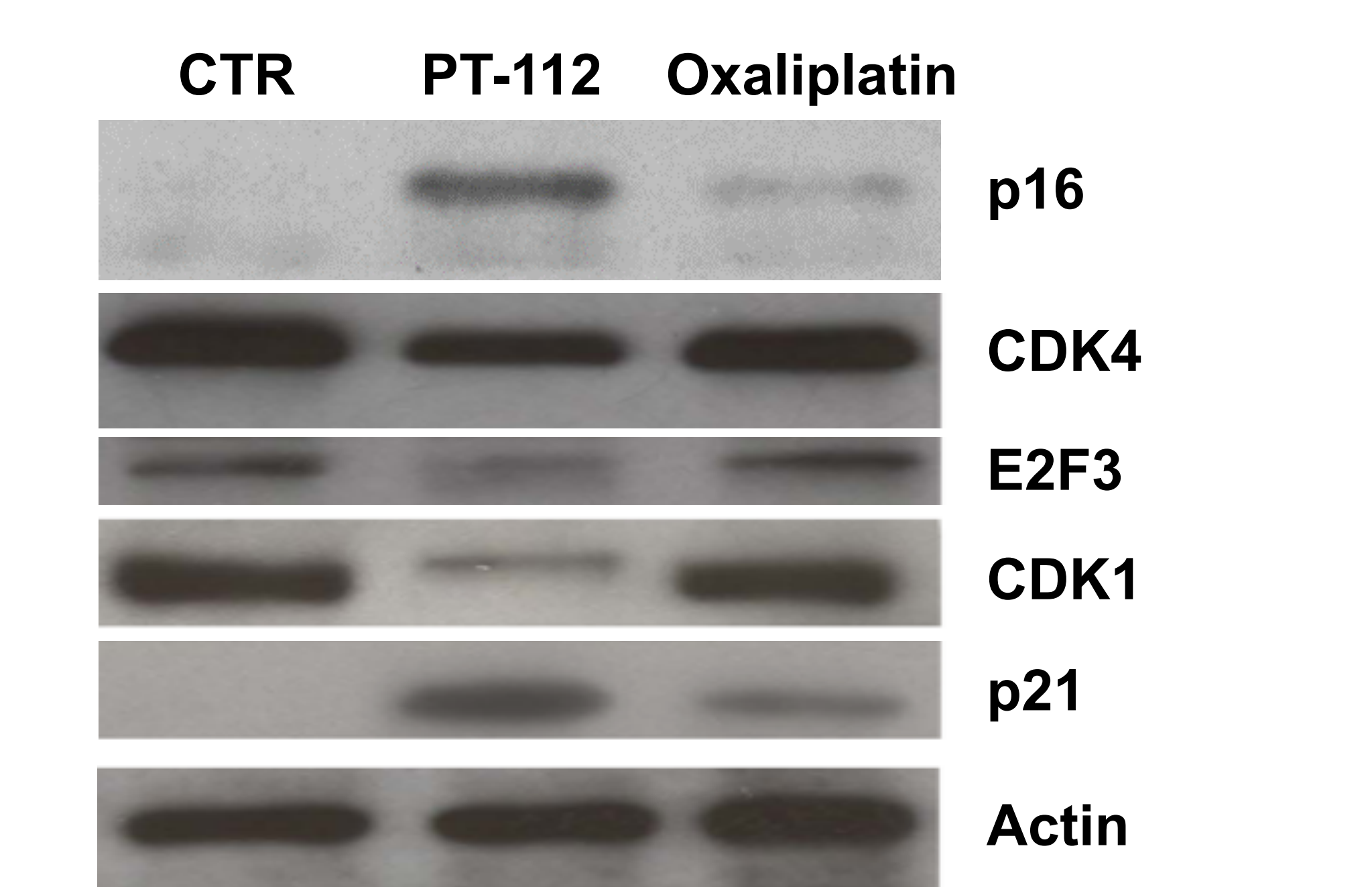


Figure 3. Cell Cycle Arrest. Western blot analysis of proteins associated with G1/S cell cycle transition after treatment with PT-112 or oxaliplatin. HCT 116 cells were exposed to each agent for 48h.

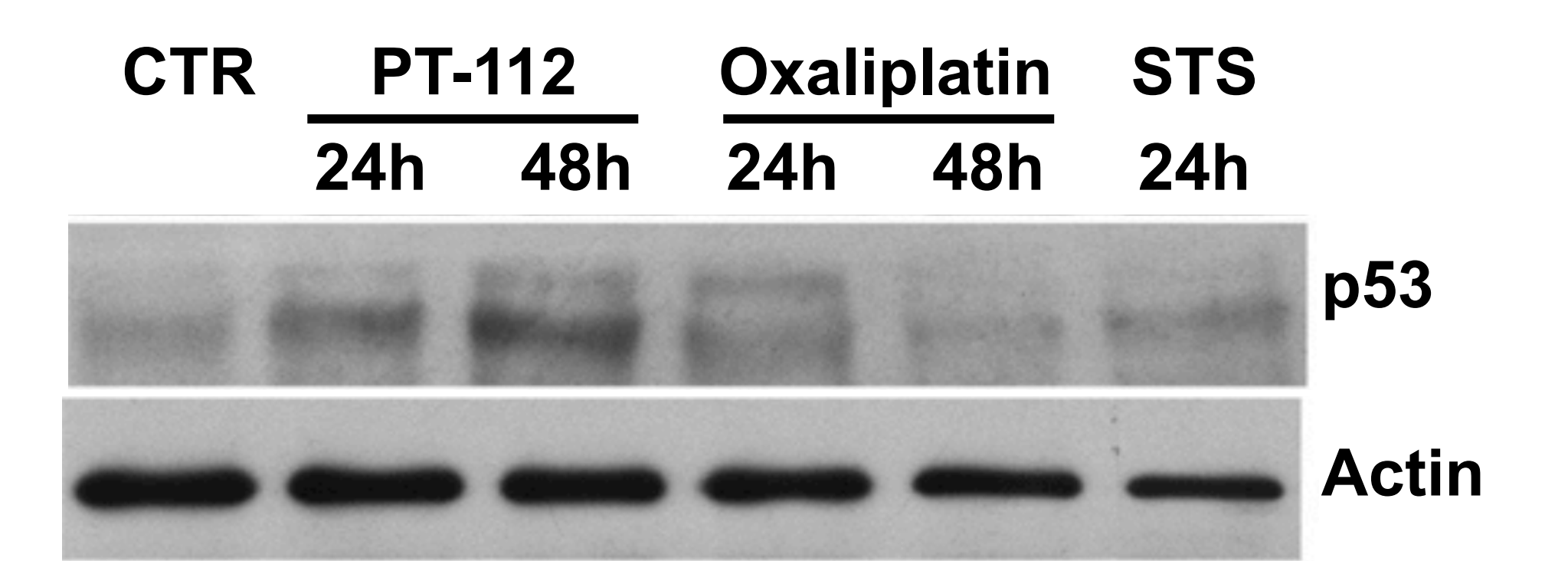


Figure 4: Increase in p53 Expression. Western blot analysis of induction of the tumor suppressor protein p53 in PT-112-treated and oxaliplatin-treated HCT 116 cells.

Apoptosis Pathway Induction

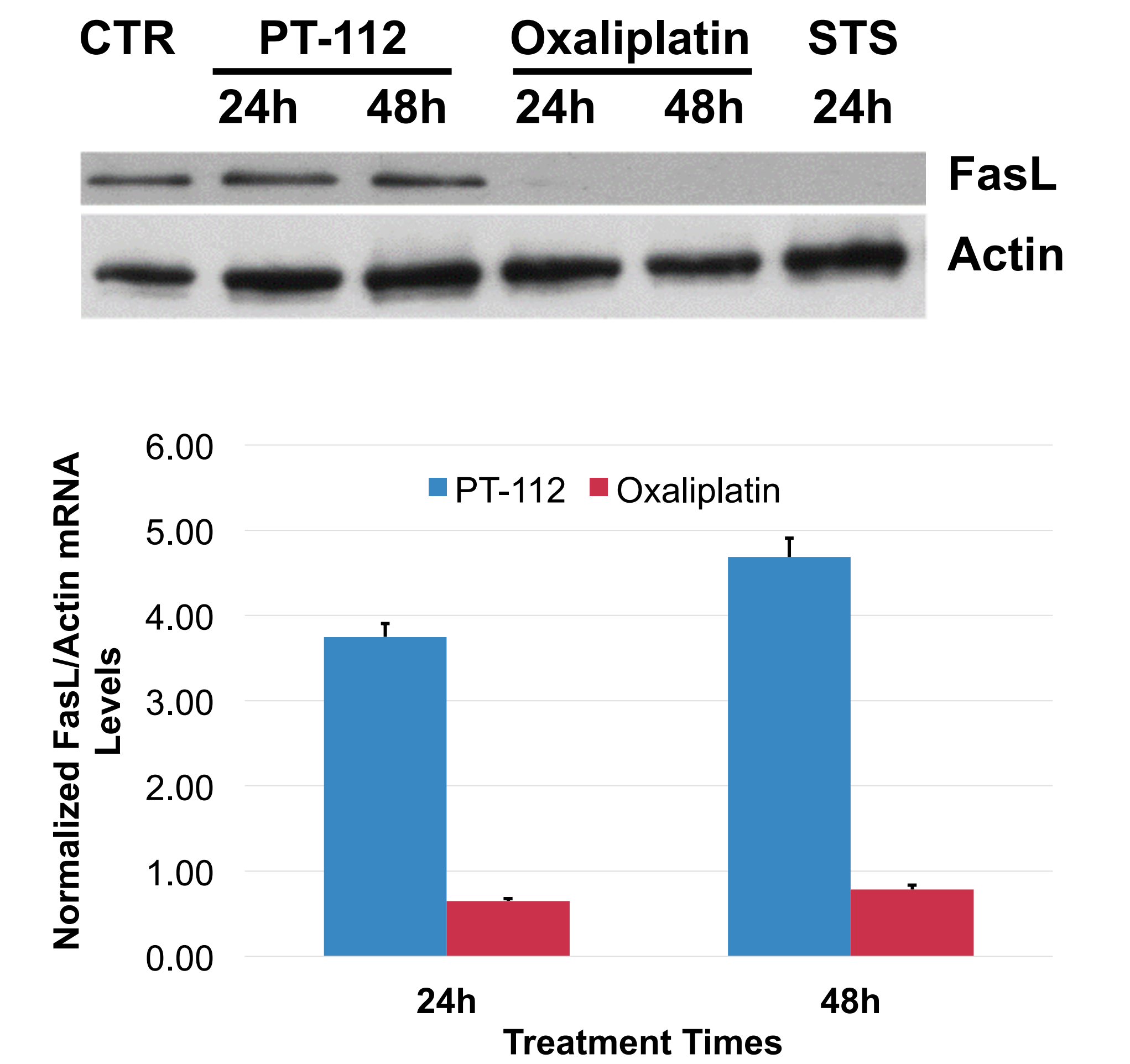


Figure 5: Induction/Suppression of FasL. Western blot (top) and qRT-PCR (bottom) analysis of induction of FasL in PT-112 and oxaliplatin treated HCT 116 cells. In the bottom figure, data were normalized to the FasL/Actin ratio of untreated cells. Error bars represent 1 SEM.

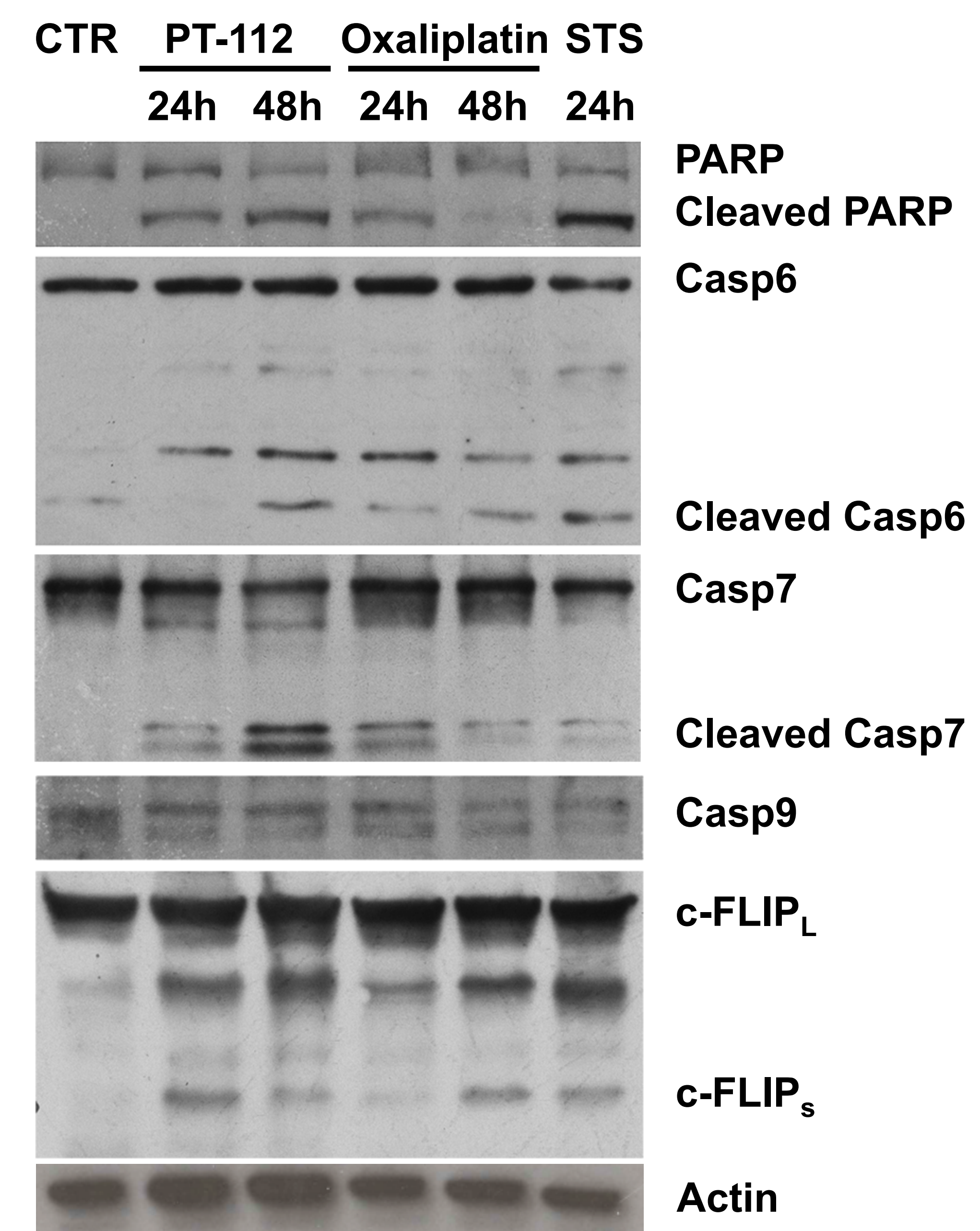


Figure 6: Induction of Apoptosis. Western blot analysis of several proteins on both the intrinsic and the extrinsic apoptotic pathways. The abbreviation Casp is used for caspase, and c-FLIP_S/c-FLIP_L for the short/long forms of cellular FLICE-like inhibitory protein, respectively.

Inhibition of NF-κB

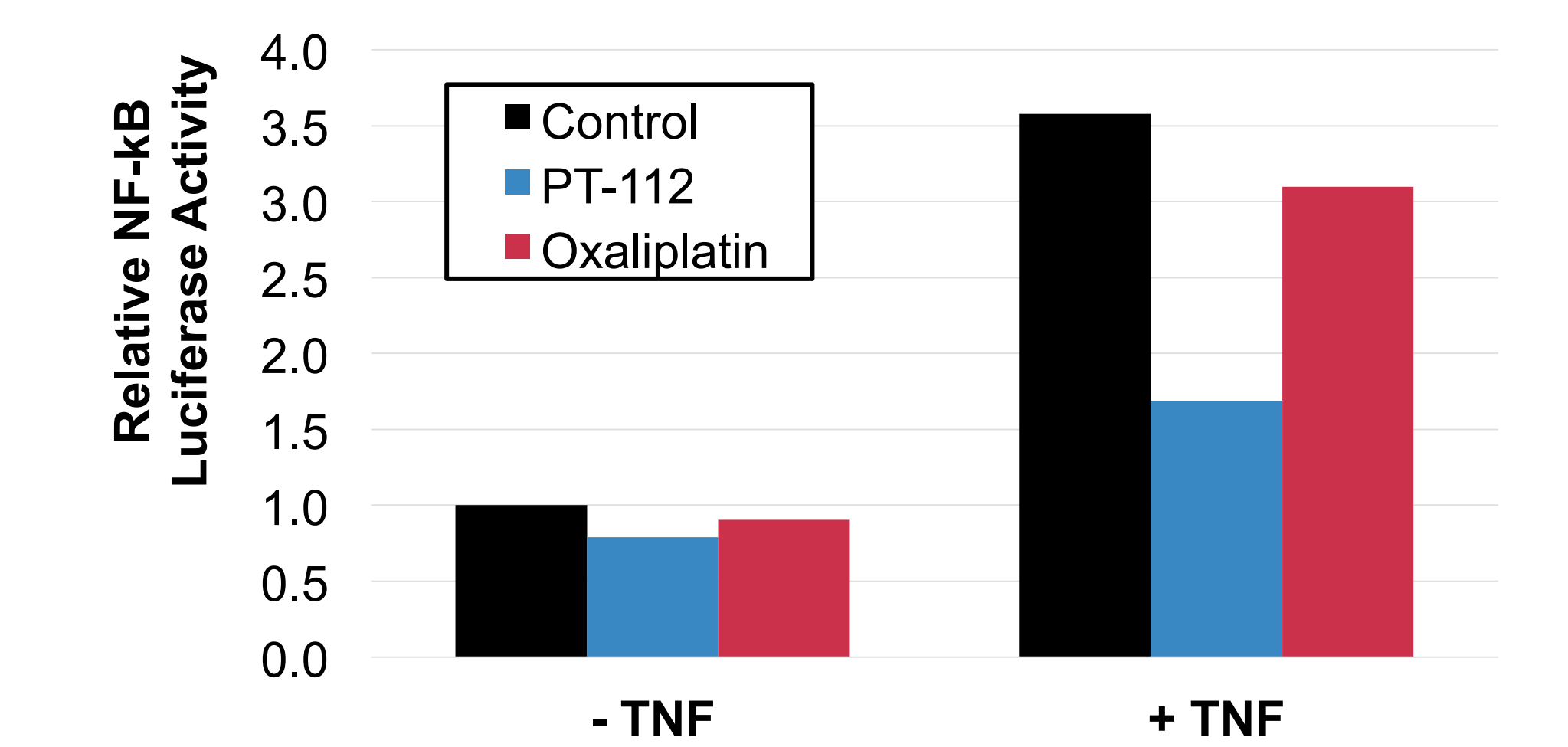


Figure 7: Inhibition of NF-κB Activity. HCT 116 cells were transfected with NF-κB reporter plasmid to measure NF-κB mediated transcription. The cells were prepared by exposing them to TNF for 15 min as indicated followed by drug treatment for 24h. The data represents the mean of two experiments performed in triplicate. Data were normalized to the TNF negative control samples.

Inhibition of Tumorigenic Phenotype

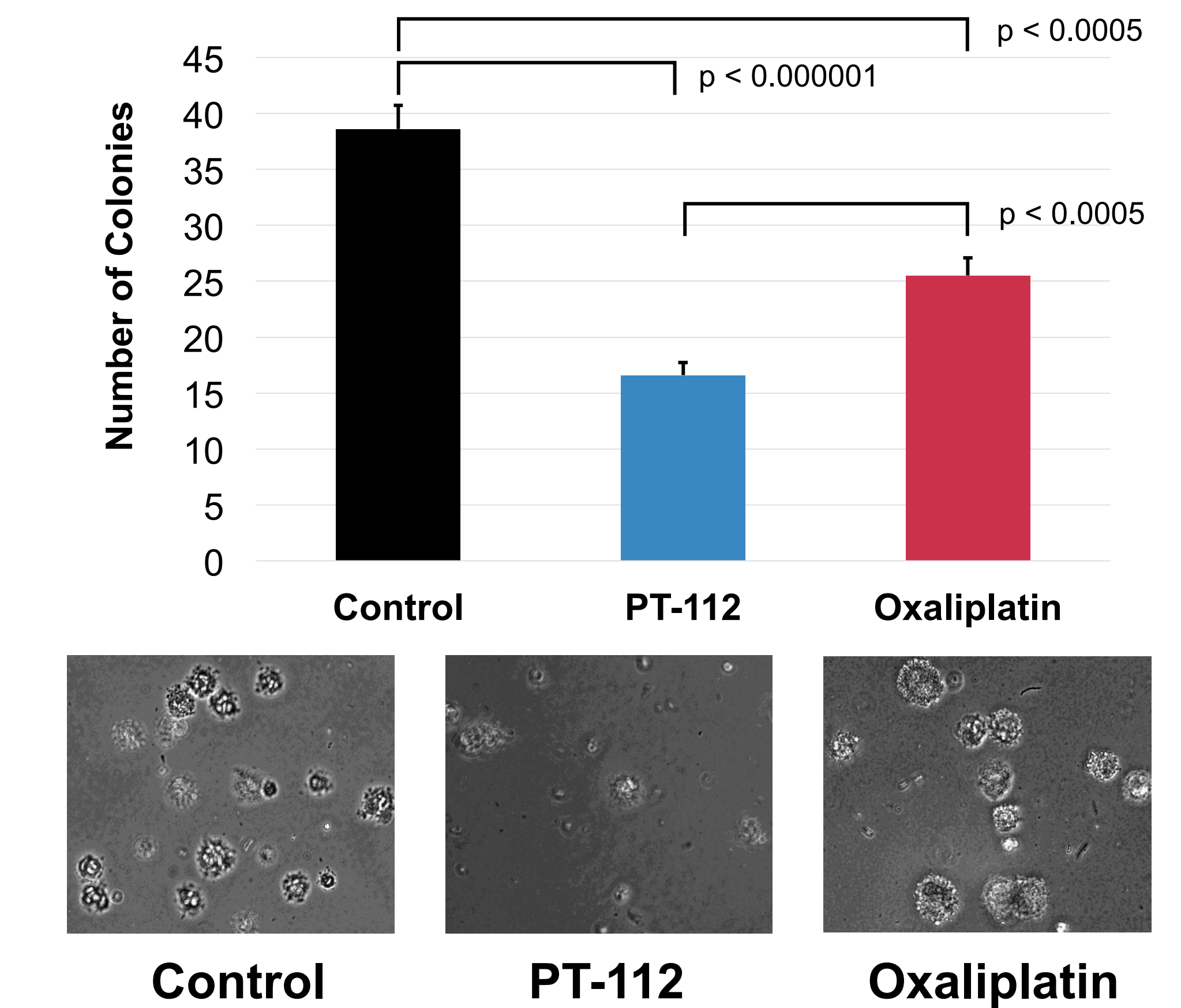


Figure 8: Evaluation of Anchorage Independent Growth. HCT 116 cells were plated in soft (0.35%) agar and treated with PT-112 or oxaliplatin for 10 days. The top shows the number of colonies formed at the conclusion of the experiment, and the bottom shows representative images of the plates. Data in top represent the average of two experiments run in quintuplicate. Error bars represent 1 SEM, and p-values were generated using two-tailed t-tests.

Effects on Non-Malignant Cells



Figure 9: Apoptosis Induction in Non-Malignant Cell line. Western blot analysis of PARP cleavage in the non-malignant colon fibroblast cell line CRL-1459. Compound concentrations were identical to those used in the HCT 116 model. In the case of PT-112 treated cells, this was not sufficient to induce apoptosis, as evidenced by the lack of PARP cleavage, and consistent with cell viability assays conducted in this cell line, including at higher concentrations (data not shown).

Immunogenic Cell Death

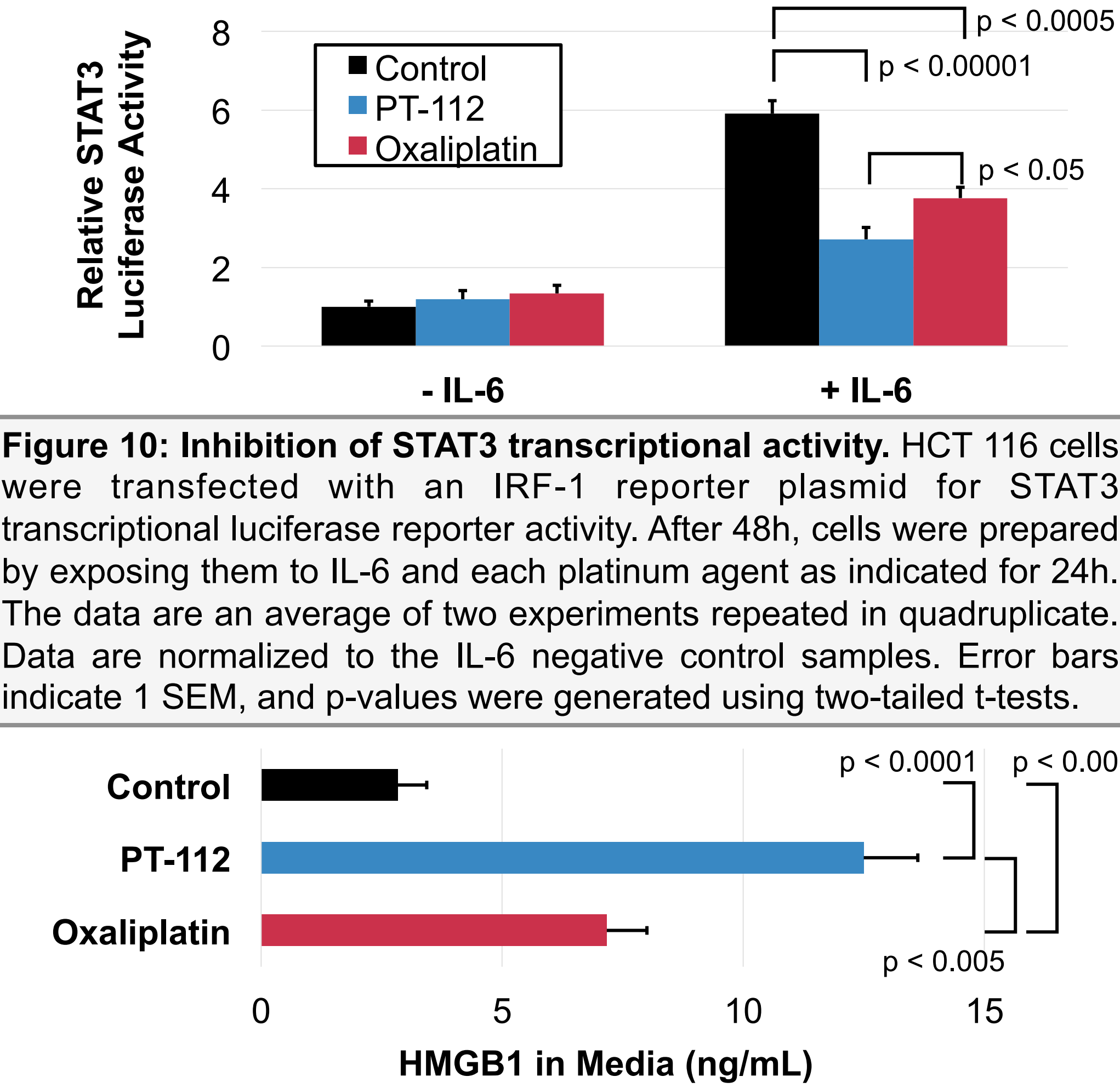


Figure 10: Inhibition of STAT3 transcriptional activity. HCT 116 cells were transfected with an IRF-1 reporter plasmid for STAT3 transcriptional luciferase reporter activity. After 48h, cells were prepared by exposing them to IL-6 and each platinum agent as indicated for 24h. The data are an average of two experiments repeated in quadruplicate. Data are normalized to the IL-6 negative control samples. Error bars indicate 1 SEM, and p-values were generated using two-tailed t-tests.

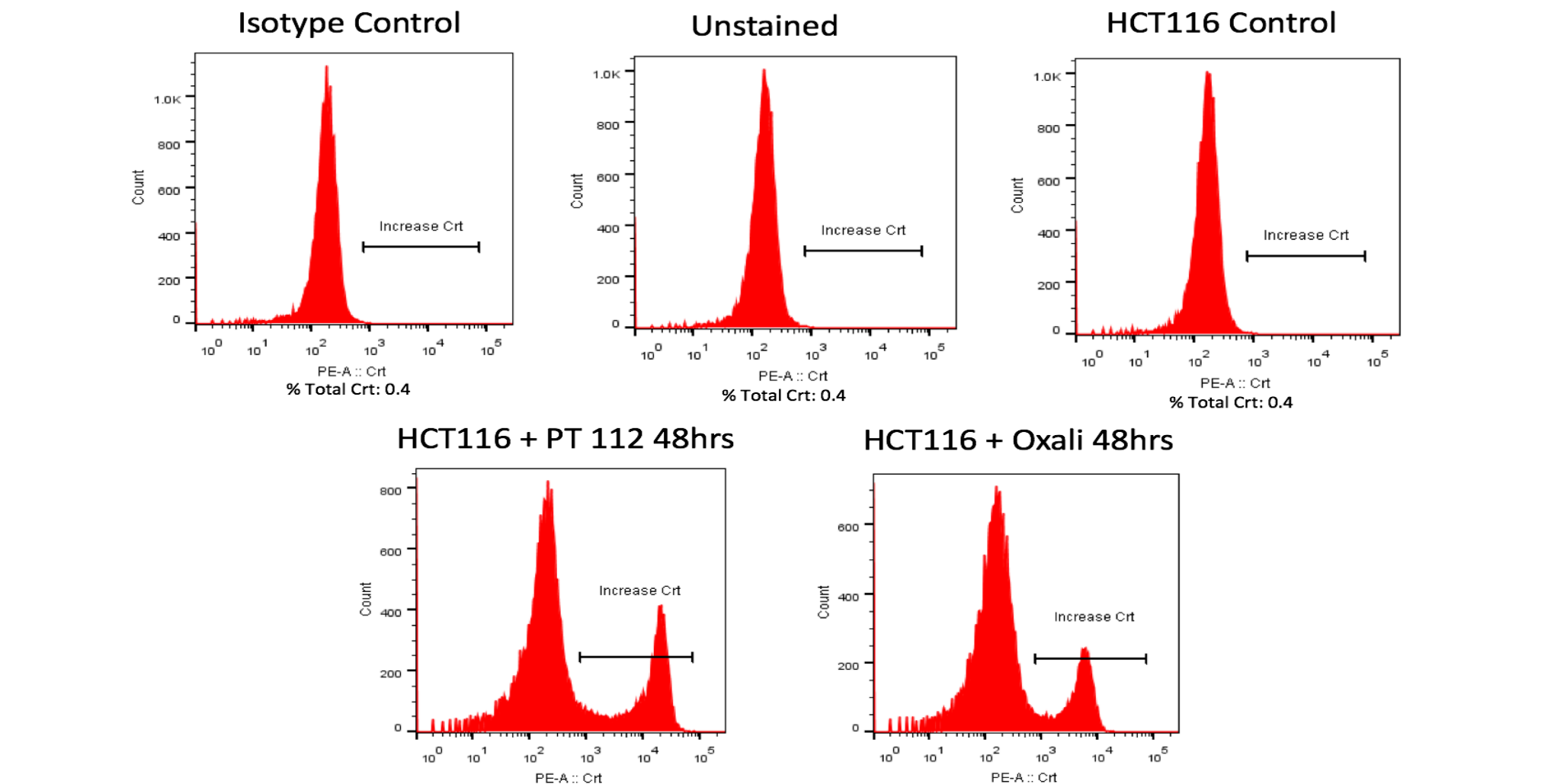


Figure 12: Cell Surface Expression of Calreticulin. Calreticulin (CRT) cell surface expression was measured via flow cytometry after 48h of PT-112 and oxaliplatin treatment. The presence of a peak to the right of the main peak indicates cells staining positive for CRT-PE, a hallmark of ICD.

Pathway Summary

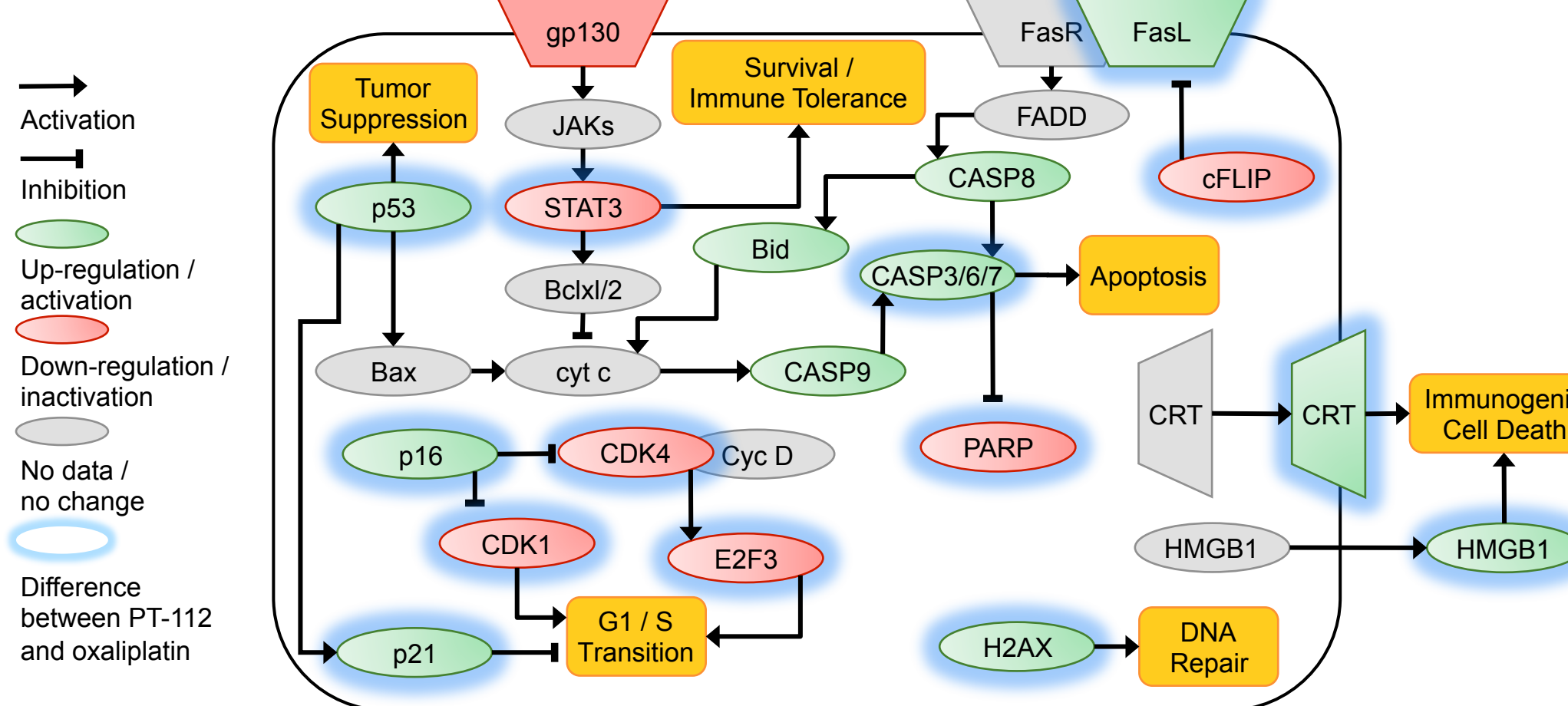


Figure 13: Summary of Findings. The large oval represents a cancer cell. The findings from the experiments conducted are represented by the shapes and coloring, per the legend at left. Arrows and blocked arrows represent simplified cancer-related cellular pathways. Fill colors indicate changes caused by PT-112 treatment.